

Water Transport through Carbon Nanotubes with the Radial Breathing Mode

Qi-Lin Zhang^{1,2}, Wei-Zhou Jiang^{1*}, Jian Liu³, Ren-De Miao⁴, Nan Sheng³

¹ Department of Physics, Southeast University, Nanjing 211189, China

² Department of Mathematics and Physics, Anhui Polytechnic University, Anhui 241000, China

³ Shanghai Institute of Applied Physics, Chinese Academy of Sciences, Shanghai 201800, China

⁴ Institute of Science, PLA University of Science and Technology, Nanjing 211101, China

Molecular dynamics simulations are performed to investigate the water permeation across the single-walled carbon nanotube (SWCNT) with the radial breathing mode (RBM) vibration. It is found that the RBM can play a significant role in breaking hydrogen bonds of the water chain, accordingly increasing the net flux dramatically, and reducing drastically the average number of water molecules inside the tube with the frequency ranging from 5000 to 11000 GHz, while far away from this frequency region the transport properties of water molecules are almost unaffected by the RBM. This phenomenon can be understood as the resonant response of the water molecule chain to the RBM. Our findings are expected to be helpful for the design of high-flux nanochannels and the understanding of biological activities especially the water channelling.

PACS numbers: 31.15.at, 31.15.xv, 61.20.Ja

Introduction—The transport properties of water molecules across nanochannels have been extensively investigated in the past [1–7]. In recent years, various designs of nanochannels concerning temperature gradients [8], charge modification [9], coulomb dragging [10], and static electric fields [11] have been proposed to study abundant novel properties of water permeation. These progresses may have significant technical implications for the design of novel nanofluidic devices or machines, such as desalination of seawater [12], molecular sieves [13], molecular water pump [14], and so on. Furthermore, one important reason why research on nanochannel transport properties has continued to be of interest is that some primary characters of water confined in simple nanochannels are similar to that of complex biological channels. Typically, water across both the biological membrane proteins (for instance, aquaporin-1 (AQP1) and Glpf) [15] and the nanochannels [16] can form single-file water chains of stable dipole orientation. The vapor-liquid transition has also been observed in mechanosensitive membrane channels [17] and other hydrophobic nanopores [18]. Another resemblance existing in the nanochannels and biological channels is that they can share both wavelike density distribution and wet-dry transition resulting from confinement [19, 20].

It has been long well-known that the wave mechanics well interprets the truth of nature. Microscopic objects such as biological microtubules are actually exposed in the environmental vibration modes of all possible micro-oscillators entangled with intrinsic modes. It is thus of broad interest to study the molecular permeations with the vibrational coherence and/or interference. Indeed, theoretical and experimental studies indicate that the single-walled carbon nanotubes (SWCNTs) have various collective vibrational modes [21–24]. Collective motion,

different from the internal fast processes, is usually regarded as the fifth dimensional motion, whereas it remains almost untouched in the study of water permeation through SWCNTs. The radial breathing mode (RBM) [25], being the simplest collective vibration, is one of the most important modes of SWCNTs, and it can be excited easily by radio wave techniques or constantly by environmental interferences. In this study, we thus restrain ourselves to the RBM. It is known that molecular dynamics (MD) simulations have been widely used to investigate the transport properties of water molecules across SWCNTs [2, 3, 16, 19, 26]. In this work, we use MD simulations to explore the dynamic behavior of water permeation through SWCNTs with the RBM. We have observed that the RBM of the SWCNT can greatly affect the water permeation properties through a resonant manner.

Computational Methods—The simulation framework is illustrated in Fig. 1. An uncapped (6,6) armchair SWCNT with a length of 1.34 nm and a diameter of 0.81 nm is embedded in two graphite sheets along the z direction. The distance between the bottom end of the SWCNT and the graphite sheet is 2 Å. Periodic boundary conditions are applied in all directions. The electrostatic calculation, carried out at a constant volume with box size dimensions of $L_x = 3.5$ nm, $L_y = 3.5$ nm, $L_z = 6.3$ nm and constant temperature (300 K) achieved by Langevin dynamics, is done using the PME [27] summation method with a cutoff for real space of 1.2 nm. The cutoff for the van der Waals interaction is also 1.2 nm. With the MD program NAMD2 [28], all simulations are performed using the CHARMM27 force field [29, 30] and the TIP3P water model [31]. The time step of 1fs is used, and data are collected every 0.5 ps. To obtain a directed flow, an additional acceleration of 0.01 nmps^{-2} , equivalent to a pressure difference about 20 Mpa between two ends of the SWCNT, is applied to each water molecule along + z direction [3, 30].

*wzjiang@seu.edu.cn

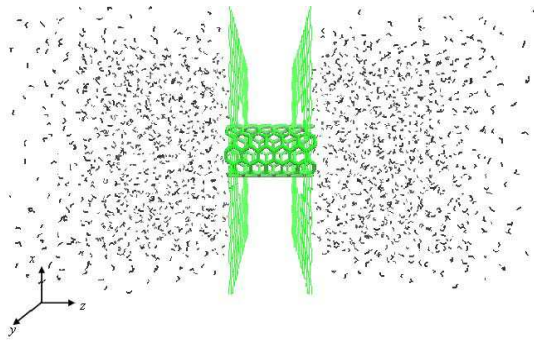


FIG. 1: (Color online) Snapshot of the simulation system. An uncapped (6,6) armchair SWCNT combined with two graphite sheets is solvated in a water box of $3.5 \times 3.5 \times 6.3 \text{ nm}^3$ with 1852 molecules. There is a vacuum between two sheets. The axis of SWCNT is parallel to the z -axis.

The RBM is simply simulated with a coherent radial motion obeying the following relation

$$r(x, y, t) = r_0(x_0, y_0, 0) + A \cos(\omega t + \varphi), \quad (1)$$

where r_0 is the equilibrium position of each carbon atom, and A is the amplitude. In the calculation, we take $\varphi = \pi/2$ and A to be 5 percent of the intersection radius. This percentage is significantly larger than the one in the literature [32–35], and we choose it for the following considerations. Though this work focuses on the RBM effect, one may be more interested in the energy transfer or molecule transport process of the microsystems induced by the more general and complex collective vibrations that involve the RBM and usually have much larger amplitudes [21, 36, 37]. On the other hand, the vibration amplitude of a biological microtubule can also be much larger [40, 41]. Specifically, we have tested that the (6,6) SWCNT is rather flexible and it is not very difficult to reach the vibration amplitude as much as 5% by appropriate external induction [38, 39]. Without losing the generality, we thus choose a moderate amplitude 5% to observe clear effects of collective vibrations and provide useful insights for the simulations of the biological microsystems. Moreover, because the filling of the water just affects the RBM frequency slightly [42], we neglect it in our estimation.

Results and Discussion— The simulation is performed for the SWCNT system with different RBM frequencies. For each frequency, the simulation time is 110 ns. Unless otherwise indicated, the data of the last 100 ns is used for analysis. For clarity, we define the net flux to be the difference between the water molecular number per nanosecond across the SWCNT from one end to the other [3, 19]. The average number [3, 16] of water molecules inside SWCNT is denoted with the symbol \bar{N} .

Fig. 2 shows the net flux and \bar{N} of water molecules across the SWCNT as a function of RBM frequency. It is observed that the net flux and \bar{N} do not change much at most frequencies and are about 20 ns^{-1} and 5,

respectively. However, as shown in Fig. 2 (inset), the net flux undergo a clear enhancement in the frequency range from about 2000 GHz to 14000 GHz, and two peak values around 4000 GHz and 12000 GHz are 63 ns^{-1} and 55 ns^{-1} , respectively, being approximately three times those beyond this frequency range. As shown in Fig. 2, we observe that the \bar{N} is around 1 in the frequency range of 5000-10000 GHz, and its minimum is about 0.84 at 6000 GHz. Water molecules inside the SWCNT are actually absent within 5000-10000 GHz in a majority of time. As an example, we have counted up the temporal distribution of the average number of water molecules inside the SWCNT in the 100 ns at 10^4 GHz. We find that the empty state, namely, no water molecule inside the tube, accounts for 46.1% of total time, and the occupancy with $\bar{N} = 1, 2, 3, 4,$ and 5 accounts for 22.5%, 14.5%, 9.9%, 5.5%, and 1.5%, respectively. Meanwhile, we have counted the hydrogen bond number of water molecules inside the SWCNT in this frequency range, according to the criterion of the oxygen distance less than 3.5 \AA and hydrogen-bond angle $\leq 30^\circ$ [19], and consistently found that it is almost always zero. Clearly, with hydrogen bonds of water molecules being almost completely broken, the water molecules move individually in the SWCNT with the RBM in this frequency range, in contrast to the existence of the single-file water chain at other frequencies. Consequently, the sharp enhancement of the flux follows from the full fracture of hydrogen bonds and fast shuttling of water molecules from one end to the other.

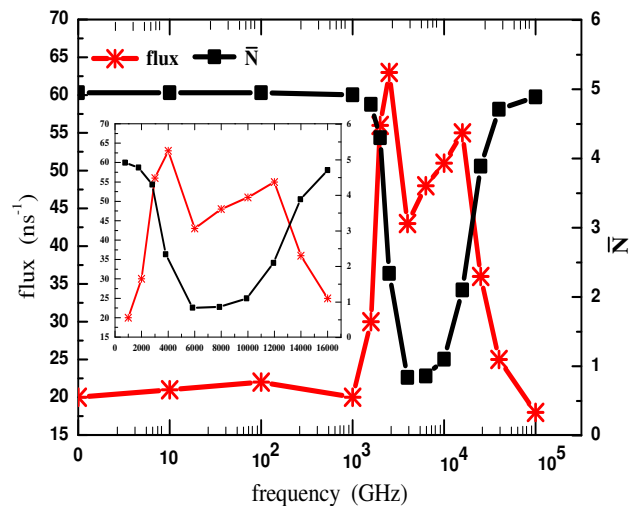


FIG. 2: (Color online) The net flux and average number \bar{N} of water molecules inside the tube as a function of RBM frequency. Given in the inset is an image amplification within the frequency interval 0-16000 GHz.

A coincident breaking of the hydrogen bonds can be realized by a perturbation of the form $e^{i\omega t}$ in sufficiently long time span, while the understanding of a thorough fracture can resort to a classical harmonic oscillator

model. Supposing the intrinsic frequency of the single-file water chain is determined by the binding energy of the hydrogen bond, E_h , we can estimate the classical resonant frequency using the relation $E_h = m\omega^2 A^2/2$ where m is the mass of water molecule, and A is the amplitude of allowed radial motion. Using the value of $E_h = 16$ kcal/mol [16] and the amplitude about 0.3-0.9 Å which are half-peak width values of the Gaussian distribution observed in the simulation, the classical resonant frequency of water chain is estimated to lie between 4800 GHz and 14500 GHz which is well situated in the frequency range for large fluxes in our simulations. It is noteworthy that the theoretical value of inherent frequency of the short (6,6) SWCNT is about 10^4 GHz [23, 32, 43, 44]. With the RBM frequency away from the resonance, segments of the water chain instead of individual molecules are produced and hence the occupancy of water molecules increases. A double-peak structure of the water flux thus appears due to the fast shuttling of the broken segments. With the RBM frequency far away from the resonance, the flux is almost unaffected by the RBM because there is just coincident breaking of hydrogen bonds. Experimentally, this drastic resonant effects on the water permeation can be verified with radio wave techniques.

To better understand the process of the hydrogen bond fracture, a dynamic evolution of the average kinetic energy of water molecules held in the tube is shown in Fig. 3. It is interesting to see that the significant fluctuation at $f = 10^4$ GHz starts to form actually at a very early time and then the shift to a strong oscillation occurs after a relatively long latent period. While this phenomenon does not take place at other frequencies as shown in Fig. 3, it can be understood as a resonant response to the RBM of the SWCNT. We note that this resonance accompanied with the H-bond rupture needs an energy accumulation process with the time span depending on the RBM amplitude.

Shown in Fig. 4 is the distance of the oxygen atom of the water molecule inside the SWCNT from the tube axis evolving with the time. Similarly, we see again that the oscillation is forced to resonate with the RBM of the SWCNT at 10^4 GHz, while the coherent oscillations do not occur at other frequencies. Posterior to the fracture of hydrogen bonds, the radial oscillation is dictated by the van der Waals interaction between the carbon atoms of the SWCNT and water molecules. It is known that the motion of water molecules is driven by the potential field. We thus calculate the average electrostatic, van der Waals and total interaction potentials: P_e , P_v and $P_t = P_e + P_v$ per water molecule at different position along z axis inside the tube where the water molecule interacts with the SWCNT, two graphite sheets, and all ambient water molecules. As shown in Fig. 5, the average interaction potentials are almost the same at all frequencies but $f = 10^4$ GHz. This explains why the net flux and \bar{N} do not have significant differences at most

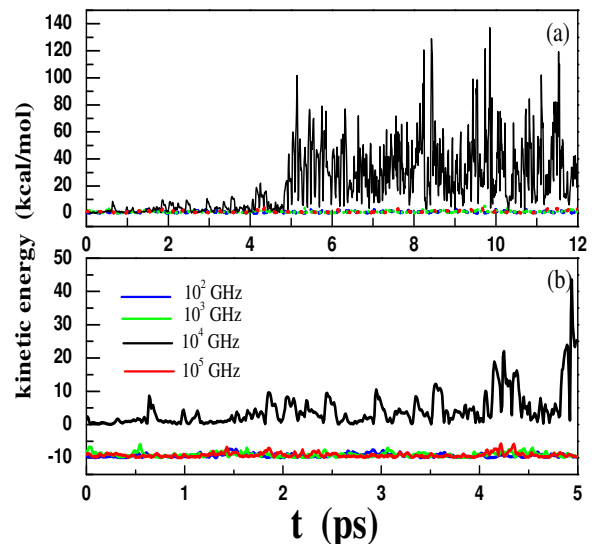


FIG. 3: (Color online) The kinetic energy for each water molecule inside the SWCNT with respect to time. Results in an earlier period are presented in the lower panel where the colored curves are displaced downwards for clarity.

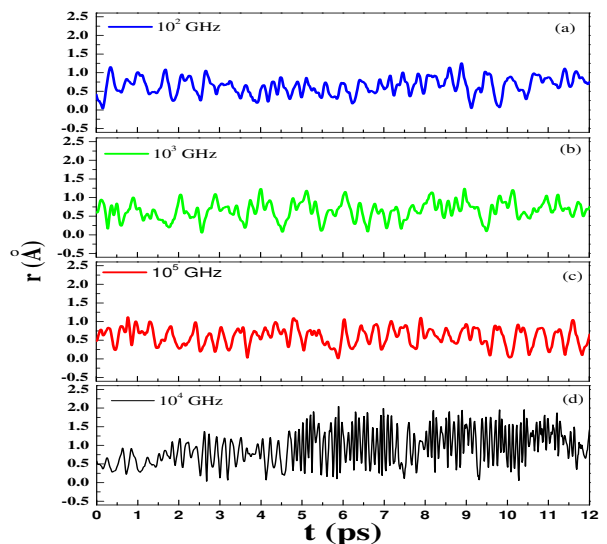


FIG. 4: (Color online) The distance of the oxygen atom of the water molecule from the z -axis evolving with time for various RBM frequencies.

frequencies. In fact, we can continuously observe stable one-dimensionally ordered water chain like previous works [3, 16, 19] using molecular visualization program VMD [45] at these frequencies. However, at 10^4 GHz, Fig. 5 (a) shows that the P_e is close to 0 kcal/mol, which means that hydrogen bonds of water molecules inside the SWCNT are almost completely deprived. Fig. 5 (b) shows that the P_v is repulsive for single water molecules, revealing the fact that the single water molecules are forced to move closely to the tube wall. The P_t , as shown in Fig. 5(c), demonstrates a similar character featured

by P_e and P_v . Due to the repulsion provided by the RBM resonance, it is difficult for water molecules to enter into and keep in the SWCNT, resulting in a dramatic reduction of \bar{N} , whereas this can indeed provide an efficient transport of water molecules accompanied by a large net flux. We mention that the peak values of the net flux do not coincide with the minimum values of \bar{N} as discussed above. On the other hand, we note that the water molecules can be as far as 2 Å from the z axis when the resonance happens (see Fig. 4). In such cases, it is necessary to explore the validity of the force-field model. With comparison to the total energy of the snapshots obtained from the ab-initio approach [46], we find that the energy acquirement of water molecules is clearly overestimated by the MD simulation. By reducing the radius parameters in the MD simulation, we may roughly reproduce the ab-initio results. In doing so, the phenomena of resonance remain unchanged, while the flux is just moderately enhanced. We observe that the H-bond fracture due to the resonant mechanism are mainly relevant to the relatively long-range van der Waals interaction in the vicinity of the equilibrium position, while the short-range repulsive interaction plays a more efficient role posterior to the H-bond fracture. Therefore, the main conclusions that we have drawn are not essentially affected by the deficiency of the MD method.

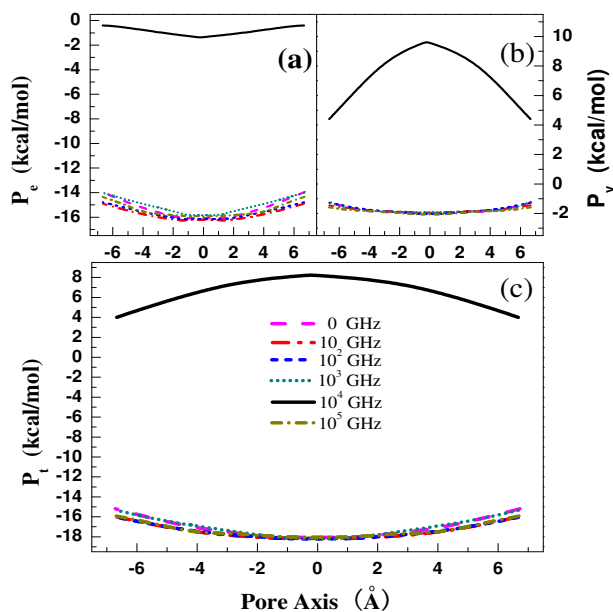


FIG. 5: (Color online) The average electrostatic (a), van der Waals (b), and total (c) potentials per water molecule that interacts with the SWCNT, two graphite sheets, and all ambient water molecules as a function of z-coordinates.

It is worth discussing the dependence of the flux on the RBM amplitude. The RBM effect on the flux decreases with the decrease of the RBM amplitude. For instance, for an amplitude of 3% of the intersection radius, the flux at $f = 10^4$ GHz reduces to be about 40 ns^{-1} which is just twice the value at frequencies without the RBM

influence. The flux enhancement can further be reduced till to disappearance at a less RBM amplitude. With the present setup, the smallest RBM amplitude is about 2.7%, while it can reduce moderately with decreasing the imposed pressure gradient.

At last, it is significant to explore the RBM effects on the water transport in SWCNTs with generalized setups that may bridge the connection with the experiments using the larger diameters and longer lengths. We have chosen the SWCNT setups with the diameter ranging from 1.09 to 1.36 nm and the length from 1.34 to 10 nm. Likewise, we have observed that the rupture of the H-bonds of various hinged water chains can occur in all these SWCNTs with the RBM at resonant frequencies, resulting in a noticeable difference in water fluxes. Moreover, we have studied the RBM effects on water transport properties at much smaller pressure gradients. It is interesting to observe that the water chain fracture is more remarkable for a small pressure gradient, e.g., 15 atm, owing to a much longer stay of water molecules in the tube. These investigations indicate that the RBM resonance is rather universal.

Conclusions—In summary, we have demonstrated effects of the resonant mechanism, responding to the RBM of the SWCNT, on the transport properties and dynamical behaviors of water molecules across the SWCNT. The resonance of the single-file water chain with the RBM of the SWCNT, characterized by the full fracture of hydrogen bonds, results in a dramatic decrease of water molecules inside the tube and a sharp enhancement of the net flux. It is also found that away from the resonance on the both sides roughly in a frequency range 2000-14000 GHz the RBM of the SWCNT can create partial breaks of hydrogen bonds and accordingly dramatic changes in transport properties of water molecules, whereas the latter are almost unaffected beyond this range. In this frequency range, a double-peak structure of the net flux forms with the vast enhancement of the net flux, and the peak values around 4000 GHz and 12000 GHz are three times those unaffected by the RBM. Our findings may have some possible implications to biological activities and potential technical applications in the development of nanotube-based nanofluidic devices.

The work was supported in part by the National Natural Science Foundation of China under Grant Nos. 10975033 and 11275048, the China Jiangsu Provincial Natural Science Foundation under Grant No.BK2009261, and Natural Science Foundation of Anhui Province of China under Grant No.1208085QA16.

-
- [1] K. Murata, K. Mitsuoka, T. Hirai, T. Walz, P. Agre, J. B. Hemann, A. Engel, and Y. Fujiyoshi, *Nature (London)* **407**, 599 (2000).
 - [2] F. Q. Zhu, E. Tajkhorshid, and K. Schulten, *Phys. Rev. Lett.* **93**, 224501 (2004).

- [3] X. J. Gong, J. Y. Li, H. J. Lu, H. Zhang, R. Z. Wan, and H. P. Fang, *Phys. Rev. Lett.* **101**, 257801 (2008); X. J. Gong, J. C. Li, K. Xu, J. F. Wang, and H. Yang, *J. Am. Chem. Soc.* **132**, 1873 (2010).
- [4] S. Joseph and N. R. Aluru, *Nano Lett.* **8**, 452 (2008).
- [5] J. Liu, J. F. Fan, M. Tang, Min Cen, J. F. Yan, Z. Liu, and W. Q. Zhou, *J. Phys. Chem. B* **114**, 12183 (2010).
- [6] W. H. Duan and Q. Wang, *ACS Nano*. **4**, 2338 (2010).
- [7] J. K. Holt *et al.*, *Science* **312**, 1034 (2006).
- [8] M. J. Longhurst and N. Quirke, *Nano Lett.* **7**, 3324 (2007).
- [9] J. Y. Li, X. J. Gong, H. J. Lu, D. Li, H. P. Fang, and R. H. Zhou, *Proc. Natl. Acad. Sci. U.S.A.* **104**, 3687 (2007).
- [10] B. Wang and P. Kra, *J. Am. Chem. Soc.* **128** 15984 (2006).
- [11] J. Y. Su and H. X. Guo, *ACS Nano*. **5**, 351 (2011).
- [12] B. Corry, *J. Phys. Chem. B* **112**, 1427 (2008).
- [13] K. B. Jirage, J. C. Hultheen, and C. R. Martin, *Science* **278**, 655 (1997).
- [14] X. J. Gong, J. Y. Li, H. J. Lu, R. Z. Wan, J. C. Li, J. Hu, and H. P. Fang, *Nat. Nanotechnol.* **2**, 709 (2007).
- [15] B. L. de Groot and H. Grubmuller, *Science* **294**, 2353 (2001).
- [16] G. Hummer, J. C. Rasaiah, and J. P. Noworyta, *Nature (London)* **414**, 188 (2001).
- [17] A. Anishkin and S. Sukharev, *Biophys. J.* **86**, 2883 (2004).
- [18] O. Beckstein and M. S. P. Sansom, *Proc. Natl. Acad. Sci. U.S.A.* **100**, 7063 (2003).
- [19] R. Z. Wan, J. Y. Li, H. J. Lu, and H. P. Fang, *J. Am. Chem. Soc.* **127**, 7166 (2005).
- [20] O. Beckstein, *et al.*, *J. Phys. Chem. B* **105**, 12902 (2001); A. V. Raghunathan and N. R. Aluru, *Phys. Rev. Lett.* **97**, 024501 (2006); P. Gallo, *et al.*, *J. Chem. Phys.* **113**, 11324 (2000); L. Kullman, *et al.*, *Biophys. J.* **82**, 803 (2002).
- [21] A. M. Rao, *et al.*, *Science*, **275**, 188 (1997).
- [22] O. Dubay and G. Kresse, *Phys. Rev. B.* **67**, 035401 (2003).
- [23] H. M. Lawler, D. Areshkin, J. W. Mintmire, and C. T. White, *Phys. Rev. B.* **72**, 233403 (2005).
- [24] W. Yang, R. Z. Wang, X. M. Song, B. Wang, and H. Yan, *Phys. Rev. B.* **75**, 045425 (2007).
- [25] P. T. Araujo, P. B. C. Pesce, M. S. Dresselhaus, K. Sato, R. Saito, and A. Jorio, *Physica E.* **42** 1251 (2010).
- [26] G. C. Zuo, R. Shen, S. J. Ma, and W. L. Guo, *ACS Nano*. **4**, 205 (2010).
- [27] T. A. Darden, D. M. York, and L. G. Pedersen, *J. Chem. Phys.* **98**, 10089 (1993).
- [28] James C. Phillips *et al.*, *J. Comput. Chem.* **26**, 1781 (2005).
- [29] A. D. MacKerell *et al.*, *J Phys Chem B* **102**, 3586 (1998).
- [30] F. Q. Zhu, E. Tajkhorshid, and K. Schulten, *Biophys. J.* **83**, 154 (2002).
- [31] W. L. Jorgensen, J. Chandrasekhar, J. D. Madura, R. W. Impey, and M. L. Klein, *J. Chem. Phys.* **79**, 926 (1983).
- [32] M. J. Longhurst and N. QUIRKE, *Molecular Simulation* **31**, 135 (2005).
- [33] N. R. Raravikar P. Keblinski, A. M. Rao, M. S. Dresselhaus, L. S. Schadler, and P. M. Ajayan, *Phys. Rev. B.* **66**, 235424 (2002).
- [34] V. P. Sokhan, D. Nicholson, and N. Quirke, *J. Chem. Phys.* **113**, 2007 (2000).
- [35] J. Küti, V. Zolyomi, M. Kertesz, and G. Sun, *New J. Phys.* **5**, 125.1 (2003).
- [36] D. Kahn and J. P. Lu, *Phys. Rev. B* **60**, 6535 (1999).
- [37] R. F. Gibson, E. O. Ayorinde, and Y. F. Wen, *Compos. Sci. and Tech.*, **67** 1 (2007).
- [38] P. Alex Greaney and Jeffrey C. Grossman, *Phys. Rev. Lett* **98**, 125503 (2007).
- [39] Ronald F. Gibson a, Emmanuel O. Ayorinde a, and Yuan-Feng Wen, *Composites Science and Technology* **67** 1 (2007).
- [40] C. Y. Wang and L. C. Zhang, *J. biomech.* **41**, 1892 (2008).
- [41] J. Pokorný, *Bioelectrochem.* **63**, 321 (2004).
- [42] S. Cambré *et al.*, *Phys. Rev. Lett.* **104**, 207401 (2010).
- [43] H. C. Cheng *et al.*, *Comput. Methods Appl. Mech. Engrg.* **199**, 2820 (2010).
- [44] S. K. Georgantzinos, G. I. Giannopoulos and N. K. Anifantis, *Comput Mech* **43**, 731 (2009).
- [45] W. Humphrey, A. Dalke, and K. Schulten, *J. Molec. Graphics* **14.1**, 33 (1996).
- [46] X. Li *et al.*, *Phys. Rev. B.* **85**, 085425 (2012).